Inorg. Chem. **2006**, *45*, 460–467

Ruthenium Mediated C–H Activation of 2-(Arylazo)phenols: Characterization of an Intermediate and the Final Organoruthenium Complex†

Parna Gupta,‡ Swati Dutta,‡ Falguni Basuli,‡ Shie-Ming Peng,§ Gene-Hsiang Lee,§ and Samaresh Bhattacharya*,‡

Department of Chemistry, Inorganic Chemistry Section, Jadavpur University, Kolkata 700 032, India, and Department of Chemistry, National Taiwan University, Taipei, Taiwan, ROC

Received October 28, 2005

Reaction of 2-(arylazo)phenols with $[Ru(PPh_3)_2(CO)_2Cl_2]$ affords a family of organometallic complexes of ruthenium(II) of type $[Ru(PPh_3)_2(CO)(CNO–R)]$, where the 2-(arylazo)phenolate ligand (CNO–R; R = OCH_3, CH_3, H, Cl, and NO_2) is coordinated to the metal center as tridentate C,N,O-donor. Another group of intermediate complexes of type $[Ru(PPh_3)_2(CO)(NO–R)(H)]$ has also been isolated, where the 2-(arylazo)phenolate ligand (NO–R) is coordinated to the metal center as bidentate N,O-donor. Structures of the $[Ru(PPh_3)_2(CO)(NO–OCH_3)(H)]$ and $[Ru(PPh_3)_2(CO)(CNO–OCH_3)]$ complexes have been determined by X-ray crystallography. All the complexes are diamagnetic and show characteristic ^1H NMR signals and intense MLCT transitions in the visible region. Both the $[Ru(PPh_3)_2(CO)(NO–R)(H)]$ and $[Ru(PPh_3)_2(CO)(CNO–R)]$ complexes show two oxidative responses on the positive side of SCE.

Introduction

There has been considerable current interest in the utilization of transition metals in promoting interesting chemical transformations of organic substrates.[1] Such reactions often proceed via a C−H activation of the organic substrate,[2] leading to the formation of a reactive organometallic intermediate, which then undergoes further reactions to yield the final product. Thus, transition metal mediated C−H activation of organic molecules is of significant importance, and the present work has originated from our interest in this area.[3] For the present study, a group of five 2-(arylazo)phenols (**1**) have been chosen as the target organic molecules, and

* To whom correspondence should be addressed. E-mail: samaresh_b@hotmail.com.

† Dedicated to Professor Animesh Chakravorty, Department of Inorganic Chemistry, Indian Association for the Cultivation of Science, Kolkata, India, on the occasion of his 70th birthday.

‡ Jadavpur University.

§ National Taiwan University.

(1) (a) Tsuji J. *Transition Metal Reagents and Catalysts*; Wiley-VCH: Weinheim, 2000. (b) Hegedus, L. S. *Coord. Chem. Rev.* **1998**, *168*, 49. (c) *Transition Metals for Organic Synthesis 1−2*; Bellar, M., Bolm, C., Eds.; Wiley-VCH: Weinheim, 1998. (d) *Applied Homogeneous Catalysis with Organometallic Compounds: A Comprehensive Handbook in Two Volumes*; Cornils, B., Hermann, W. A., Eds.; VCH: Weinheim, 1996. (e) *Advances in Metal-Organic Chemistry*; Liebeskind, L. S., Ed.; JAI Press: Greenwich, CT, 1996. (f) *Comprehensive Organometallic Chemistry*; Abel, E., Stone, F. G. A., Wilkinson, G., Eds.; Pergamon Press: Oxford, 1995; Vol. 12. (g) Hegedus, L. S. *Transition Metals in the Synthesis of Complex Organic Molecules*; University Science Books: Mill Valley, CA, 1994. (h) Collman, J. P.; Hegedus, L. S.; Norton, J. R.; Finke, R. G. *Principles and Applications of Organotransition Metal Chemistry*; University Science Books: Mill Valley, CA, 1987. (i) Trost, B. M.; Verhoeven, T. R. *Comprehensive Organometallic Chemistry*; Abel, E., Stone, F. G. A., Wilkinson, G., Eds.; Pergamon Press: Oxford, 1982, *8*.

(2) (a) Jaeger-Fiedle, U.; Arndt, P.; Baumann, W.; Spannenberg, A.; Burlakov, V. V.; Rosenthal, U. *Eur. J. Inorg. Chem.* **2005**, *14*, 2842. (b) Keuseman, K. J.; Smolinkova, I. P.; Dunina, V. V. *Organometallics* **2005**, *24*, 4159. (c) Shi, L.; Tu, Y. Q.; Wang, M.; Zhao, F. M.; Fan, C. A.; Zhao, Y. M.; Xia, W. J. *J. Am. Chem. Soc.* **2005**, *127*, 10836. (d) Thalji, R. K.; Ahrendt, K. A.; Bergman, R. G.; Ellman, J. A. *J. Org. Chem*. **2005**, *70*, 6775. (e) Fan, Y.; Hall, M. B. *Organometallics* **2005**, *24*, 3827. (f) Esteruelas, M. A.; Lopez, A. M. *Organometallics* **2005**, *24*, 3584. (g) Driver, T. G.; Day, M. W.; Labinger, J. A.; Bercaw, J. E. *Organometallics* **2005**, *24*, 3644. (h) Rybtchinski, B.; Cohen, R.; Jan, M. L.; Milstein, D. *J. Am. Chem. Soc.* **2003**, *125*, 11041. (i) Pamplin, C. B.; Legzdins, P. *Acc. Chem. Res.* **2003**, *36*, 223. (j) Ritleng, V.; Sirlin, C.; Pfeffer, M. *Chem. Rev.* **2002**, *102*, 1731. (k) Rybtchinski, B.; Oevers, S.; Montag, M.; Vigalok, A.; Rozenberg, A.; Martin, J. M. L.; Milstein, D. *J. Am. Chem. Soc.* **2001**, *123*, 9064. (l) Vigalok, A.; Milstein, D. *Acc. Chem. Res.* **2001**, *34*, 798. (m) Slugovc, C.; Padilla-Martnez, I.; Sirol, S.; Carmona, E. *Coord. Chem. Rev.* **2001**, *213*, 129. (n) Jia, C.; Kitamura, T.; Fujiwara, Y. *Acc. Chem. Res.* **2001**, *34*, 633. (o) Sundermann, A.; Uzan, O.; Milstein, D.; Martin, J. M. L. *J. Am. Chem. Soc.* **2000**, *122*, 7095.

10.1021/ic051874v CCC: $33.50
Published on Web 12/01/2005

ruthenium has been selected as the transition metal for promoting the C−H activation. The 2-(arylazo)phenols are

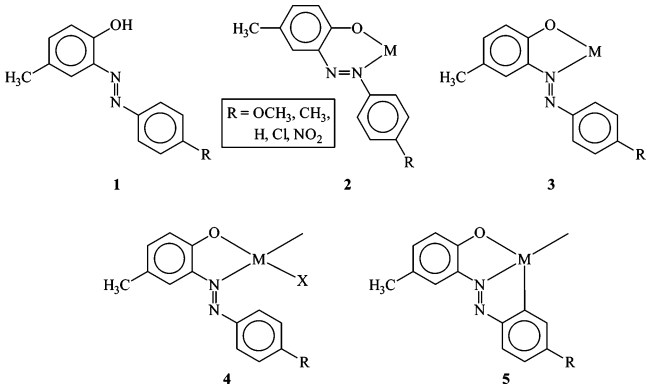

known to bind to metal ions usually as bidentate N,O-donors, via dissociation of the phenolic proton, forming a six-membered chelate ring (**2**).[4] However, in a recent study the 2-(arylazo)phenols have been observed to coordinate the metal center as bidentate N,O-donors forming a stable five-membered chelate ring (**3**).[5] In the solid state the pendent phenyl ring in the arylazo fragment in **3** is observed to remain almost orthogonal to the plane of the chelate ring. However, in view of the possible rotation of this phenyl ring around the C−N bond in the solution phase, and particularly in view of the resulting closeness of the phenyl ring to the metal center when it becomes coplanar with the chelate ring, C−H activation at the ortho position of the phenyl ring appears to be a possibility. A necessary prerequisite for such speculated C−H activation to occur is the existence of a potentially labile ligand (X) trans to the phenolate oxygen (**4**), which would facilitate the targeted C−H activation leading to the formation of the corresponding orthometalated species (**5**) via elimination of HX. With this strategy in mind, [Ru(PPh$_3$)$_2$(CO)$_2$Cl$_2$] has been selected as the ruthenium starting material. This particular complex has been picked up because of its demonstrated ability to accommodate monoanionic bidentate (L−L) ligands via displacement of one CO and one chloride,[3d] and hence, it is expected to provide a labile Ru−Cl bond in the equatorial plane containing the Ru(L−L)(CO)Cl fragment, as required for the targeted C−H activation. Reaction of the 2-(arylazo)phenols (**1**) with [Ru(PPh$_3$)$_2$(CO)$_2$Cl$_2$] has indeed afforded a family of organoruthenium complexes, where the 2-(arylazo)phenols are coordinated as in **5**. In addition, a group of complexes of another type could also be isolated from the same reaction. The present report deals with the chemistry of all these complexes, with special reference to their formation, structure, and spectral and electrochemical properties.

Experimental Section

Materials. Commercial ruthenium trichloride was purchased from Arora Matthey, Kolkata, India. The *para*-substituted anilines and *p*-cresol were obtained from S.D, India. All other chemicals and solvents were reagent grade commercial materials and were used as received. [Ru(PPh$_3$)$_2$(CO)$_2$Cl$_2$] was synthesized by following a reported procedure.[6] The 2-(arylazo)phenol ligands were prepared by coupling diazotized *para*-substituted anilines with *para*-cresol. Purification of dichloromethane and acetonitrile and preparation of tetrabutylammonium perchlorate (TBAP) for electrochemical work were performed as reported in the literature.[7]

Preparations of Complexes. [Ru(PPh$_3$)$_2$(CO)(NO−R)(H)] and [Ru(PPh$_3$)$_2$(CO)(CNO−R)]. The [Ru(PPh$_3$)$_2$(CO)(NO−R)(H)] and [Ru(PPh$_3$)$_2$(CO)(CNO−R)] complexes were obtained by following a general procedure. Specific details are given below for a particular complex.

[Ru(PPh$_3$)$_2$(CO)(NO−H)(H)] and [Ru(PPh$_3$)$_2$(CO)(CNO−H)]. 2-(Phenylazo)-4-methylphenol (30 mg, 0.14 mmol) was dissolved in ethanol (40 mL), and [Ru(PPh$_3$)$_2$(CO)$_2$Cl$_2$] (100 mg, 0.14 mmol) was added to it. The mixture was then refluxed for 6 h to yield a red solution. The solvent was evaporated, and the solid mass, thus obtained, was subjected to purification by thin-layer chromatography on a silica plate. With 1:1 hexane−benzene as the eluant, a red band and a green band separated, and the corresponding materials were extracted separately with acetonitrile. Evaporation of these acetonitrile extracts gave [Ru(PPh$_3$)$_2$(CO)(NO−H)(H)] and [Ru(PPh$_3$)$_2$(CO)(CNO−H)] as red and green crystalline solids, respectively. Yields: 45% and 50%, respectively.

[Ru(PPh$_3$)$_2$(CO)(CNO−R)]. The [Ru(PPh$_3$)$_2$(CO)(CNO−R)] complexes were also prepared by following two different procedures, which are described below for a specific complex.

[Ru(PPh$_3$)$_2$(CO)(CNO−H)]. Method A. 2-(Phenylazo)-4-methylphenol (30 mg, 0.14 mmol) was dissolved in 2-methoxyethanol (40 mL), and [Ru(PPh$_3$)$_2$(CO)$_2$Cl$_2$] (100 mg, 0.14 mmol) was added to it. The mixture was then refluxed for 6 h to yield a greenish brown solution. The solvent was evaporated, and the solid residue, thus obtained, was purified by thin-layer chromatography on a silica plate. With 1:1 hexane−benzene as the eluant, a green band separated, and the corresponding material was extracted with acetonitrile. Evaporation of the acetonitrile extract gave [Ru(PPh$_3$)$_2$(CO)(CNO−H)] as a green crystalline solid. Yield: 70%.

Method B. The red [Ru(PPh$_3$)$_2$(CO)(NO−H)(H)] complex (100 mg, 0.12 mmol) was taken in 2-methoxyethanol (50 mL). The solution was heated at reflux for 10 min, whereby it turned green. Evaporation of the solvent afforded [Ru(PPh$_3$)$_2$(CO)(CNO−H)] as a green crystalline solid. Yield: quantitative.

Anal. Calcd for [Ru(PPh$_3$)$_2$(CO)(NO−OCH$_3$)(H)]: C, 68.10; H, 4.77; N, 3.17. Found: C, 68.83; H, 4.72; N, 3.10. ^{1}H NMR:[8] −10.5 (t, hydride, J = 22.0); 2.11 (CH$_3$); 3.57 (OCH$_3$); 6.31 (d, 1H, J =

(3) (a) Nag, S.; Gupta, P.; Butcher, R. J.; Bhattacharya S. *Inorg. Chem.* **2004**, *43*, 4814. (b) Acharyya, R.; Basuli, F.; Wang, R. Z.; Mak, T. C. W.; Bhattacharya, S. *Inorg. Chem.* **2004**, *43*, 704. (c) Pal, I.; Dutta, S.; Basuli, F. Goverdhan, S.; Peng, S. M.; Bhattacharya, S. *Inorg. Chem.* **2003**, *42*, 4338. (d) Basuli, F.; Peng, S. M.; Bhattacharya, S. *Inorg. Chem.* **2001**, *40*, 1126. (e) Majumder, K.; Peng, S. M.; Bhattacharya, S. *J. Chem. Soc., Dalton Trans.* **2001**, 284. (f) Basuli, F.; Peng, S. M.; Bhattacharya, S. *Inorg. Chem.* **2000**, *39*, 1120. (g) Dutta, S.; Peng, S. M.; Bhattacharya, S. *J. Chem. Soc., Dalton Trans.* **2000**, 4623.

(4) (a) Rath, R. K.; Nethaji, M.; Chakravarty, A. R. *J. Organomet. Chem.* **2001**, *633*, 79. (b) Sui, K.; Peng, S. M.; Bhattacharya, S. *Polyhedron* **1999**, *19*, 631. (c) Bhawmik, R.; Biswas, H.; Bandyopadhyay, P. *J. Organomet. Chem.* **1995**, *498*, 81. (d) Sinha, C. R.; Bandyopadhyay, D.; Chakravorty, A. *J. Chem. Soc., Chem. Commun.* **1988**, 468. (e) Dyachenko, O. A.; Atovmyan, L. O.; Aldosin, S. M. *J. Chem. Soc., Chem. Commun.* **1975**, 105. (f) Kalia, K. C. *Indian J. Chem.* **1970**, *8*, 1035. (g) Price, R. J. *J. Chem. Soc. A* **1969**, 1296. (h) Jarvis, J. A. J. *Acta Crystallogr.* **1961**, *14*, 961.

(5) Basuli, F.; Peng, S. M.; Bhattacharya, S. *Polyhedron* **1998**, *18*, 391.

(6) Ahmad, N.; Robinson, S. D.; Uttley, M. F. *J. Chem. Soc., Dalton Trans.* **1972**, 843.

(7) (a) Sawyer, D. T.; Roberts, J. L., Jr. *Experimental Electrochemistry for Chemists*; Wiley: New York, 1974; pp 167−215. (b) Walter, M.; Ramaley, L. *Anal. Chem.* **1973**, *45*, 165.

6.0); 6.36 (s, 1H); 7.10−7.90 (2PPh_3); 7.55−7.57 (d, 2H).* ^{13}C NMR: 19.72 (s, CH_3); 44.54 (s, OCH_3); 127.47 (t, PPh_3, J = 17.85); 129.11(s, PPh_3); 131.86 (t, PPh_3, J = 27.30); 133.83 (t, PPh_3, J = 23.68); 100.15, 101.91, 115.38, 121.34, 123.98, 125.50, 127.44, 131.45, 133.33, 144.40, 153.12, and 161.44 (phenyl carbons of NO−OCH_3 ligand); 202.20 (s, CO). ^{31}P NMR: 41.13 (s, 2PPh_3). IR: 1928 cm^{-1} (ν_{CO}).

Anal. Calcd for [Ru(PPh_3)$_2$(CO)(NO−CH_3)(H)]: C, 68.60; H, 5.01; N, 3.18. Found: C, 68.77; H, 5.04; N, 3.24. ^{1}H NMR:[8] −10.50 (t, hydride, J = 22.0); 2.10 (CH_3); 2.30 (CH_3); 6.91 (d, 1H, J = 9.0); 7.07 (s, 1H); 7.30−7.87 (2PPh_3); 7.11 (d, 1H, J = 6.0); 7.54 (d, 1H, J = 6.0). ^{13}C NMR: 19.71 (s, CH_3); 20.01 (s, CH_3); 127.47 (t, PPh_3, J = 18.20); 129.11(s, PPh_3); 131.86 (t. PPh_3, J = 27.45); 133.83 (t, PPh_3, J = 23.59); 106.54, 108.71, 117.88, 122.34, 125.88, 127.55, 129.44, 134.44, 137.43, 148.41, 155.12, and 169.50 (phenyl carbons of NO−CH_3 ligand); 202.33 (s, CO). ^{31}P NMR: 41.22 (s, 2PPh_3). IR: 1930 cm^{-1} (ν_{CO}).

Anal. Calcd for [Ru(PPh_3)$_2$(CO)(NO−H)(H)]: C, 69.36; H, 4.85; N, 3.23. Found: C, 69.45; H, 5.02; N, 3.60. ^{1}H NMR:[8] −10.67 (t, hydride, J = 22.0); 2.10 (CH_3); 6.02 (d, 1H, J = 9.0); 6.43 (d, 1H, J = 9.0); 6.58 (d, 1H, J = 9.0); 6.93 (t, 1H, J = 9); 7.05 (t, 1H, J = 7.5); 7.15 (s, 1H); 7.10−7.90 (2PPh_3). ^{13}C NMR: 19.74 (CH_3); 127.53 (t, PPh_3, J = 18.00); 129.11(s, PPh_3); 131.86 (t, PPh_3, J = 27.30); 133.83 (t, PPh_3, J = 23.70); 116.54, 119.91, 121.38, 122.34, 125.98, 127.47, 128.24, 133.45, 134.23, 146.46, 157.02, and 171.50 (phenyl carbons of NO−H ligand); 202.40 (s, CO). ^{31}P NMR: 41.19 (s, 2PPh_3). IR: 1928 cm^{-1} (ν_{CO}).

Anal. Calcd for [Ru(PPh_3)$_2$(CO)(NO−Cl)(H)]: C, 66.70; H, 4.56; N, 3.11. Found: C, 66.97; H, 4.64; N, 3.42.^{1}H NMR:[8] −10.61 (t, hydride, J = 22.0); 2.11 (CH_3); 6.00 (d, 1H, J = 6.0); 6.28 (d, 1H, J = 6.0); 7.10 (s, 1H); 7.20−7.52 (2PPh_3). ^{13}C NMR: 19.67 (CH_3); 127.47 (t, PPh_3, J = 18.30); 129.11(s, PPh_3); 131.86 (t, PPh_3, J = 27.57); 133.83 (t, PPh_3, J = 23.72); 122.54, 124.81, 127.38, 130.44, 132.78, 136.50, 138.34, 140.15, 153.23, 161.40, 178.12, and 185.45 (phenyl carbons NO−Cl ligand); 202.38 (s, CO). ^{31}P NMR: 41.20 (s, 2PPh_3). IR: 1931 cm^{-1} (ν_{CO}).

Anal. Calcd for [Ru(PPh_3)$_2$(CO)(NO−NO_2)(H)]: C, 65.93; H, 4.50; N, 4.62. Found: C, 66.00; H, 4.45; N, 4.33. ^{1}H NMR:[8] −10.36 (t, hydride, J = 22.0); 2.12 (CH_3); 5.96 (d, 1H, J = 9.0); 6.30 (d, 1H, J = 9.0); 6.60 (d, 1H, J = 9.0); 7.19 (s, 1H); 7.18−7.40 (2PPh_3). ^{13}C NMR: 19.70 (CH_3); 127.47 (t, PPh_3, J = 18.15); 129.11(s, PPh_3); 131.86 (t, PPh_3, J = 27.45); 133.83 (t, PPh_3, J = 23.74); 125.54, 128.71, 133.18, 139.64, 142.28, 148.50, 156.14, 162.15, 163.23, 167.50, 180.42, and 189.50 (phenyl carbons of NO−NO_2 ligand); 202.29 (s, CO). ^{31}P NMR: 40.99 (s, 2PPh_3). IR: 1930 cm^{-1} (ν_{CO}).

Anal. Calcd for [Ru(PPh_3)$_2$(CO)(CNO−OCH_3)]: C, 68.53; H, 4.70; N, 3.14. Found: C, 68.78; H, 4.44; N, 2.92. ^{1}H NMR:[8] 2.07 (CH_3); 3.67 (OCH_3); 6.03 (d, 1H, J = 9.0); 6.39 (d, 1H, J = 9.0); 6.53−6.61 (3H);* 7.07 (s, 1H), 7.22−7.49 (2PPh_3). ^{13}C NMR: 29.71 (s, CH_3); 54.83 (s, OCH_3); 127.71 (t, PPh_3, J = 16.83); 129.52 (s, PPh_3); 132.06 (t, PPh_3, J = 27.88); 134.02 (t, PPh_3, J = 22.30); 108.96, 115.80, 120.97, 124.10, 126.16, 127.52, 128.25, 133.84, 134.37, 158.16, and 161.20 (phenyl carbons of CNO−OCH_3 ligand); 179.59 (metalated carbon); 208.31 (s, CO). ^{31}P NMR: 31.00 (s, 2PPh_3). IR: 1922 cm^{-1} (ν_{CO}).

Anal. Calcd for [Ru(PPh_3)$_2$(CO)(CNO−CH_3)]: C, 69.78; H, 4.79; N, 3.19. Found: C, 69.92; H, 4.32; N, 2.94. ^{1}H NMR:[8] 1.88 (CH_3); 1.80 (CH_3); 5.93 (d, 1H, J = 9.0); 6.04 (s, 1H); 6.35 (d, 1H, J = 9.0); 6.67 (s, 1H); 7.16−7.36 (2PPh_3). ^{13}C NMR: 29.69 (s, CH_3); 30.83 (s, CH_3); 127.71 (t, PPh_3, J = 16.80); 129.52 (s, PPh_3); 131.96 (t, PPh_3 J = 27.80); 134.02 (t, PPh_3, J = 22.20); 110.29, 118.20, 123.27, 127.50, 129.46, 130.22, 132.25, 137.14, 138.57, 162.06, and 166.00 (phenyl carbons of CNO−CH_3 ligand); 180.50 (metalated carbon); 208.27 (s, CO). ^{31}P NMR: 30.99 (s, 2PPh_3). IR: 1920 cm^{-1} (ν_{CO}).

Anal. Calcd for [Ru(PPh_3)$_2$(CO)(CNO−H)]: C, 69.52; H, 4.63; N, 3.24. Found: C, 69.47; H, 4.77; N, 3.22. ^{1}H NMR:[8] 2.10 (CH_3); 5.50 (d, 1H, J = 9.0); 5.95 (s, 1H); 6.25−6.35 (2H);* 7.07−7.25 (2PPh_3). ^{13}C NMR: 29.68 (s, CH_3); 127.71 (t, PPh_3, J = 16.85); 129.52 (s, PPh_3); 132.06 (t, PPh_3, J = 27.76); 134.02 (t, PPh_3, J = 22.30); 116.66, 124.10, 129.97, 132.20, 134.46, 135.52, 137.20, 143.84, 144.87, 162.16, and 168.20 (phenyl carbons of CNO−H ligand); 181.09 (metalated carbon); 208.30 (s, CO). ^{31}P NMR: 31.10 (s, 2PPh_3). IR: 1922 cm^{-1} (ν_{CO}).

Anal. Calcd for [Ru(PPh_3)$_2$(CO)(CNO−Cl)]: C, 66.85; H, 4.34; N, 3.11. Found: C, 66.65; H, 4.27; N, 3.45. ^{1}H NMR:[8] 2.05 (CH_3); 5.01 (d, 1H, J = 9.0); 5.85 (s, 1H); 6.25 (d, 1H, J = 9.0); 6.50 (s, 1H); 7.30−7.60 (2PPh_3). ^{13}C NMR: 29.67 (s, CH_3); 127.71 (t, PPh_3, J = 16.78); 129.52 (s, PPh_3); 132.06 (t, PPh_3, J = 27.83); 134.02 (t, PPh_3, J = 22.20); 120.96, 128.00, 133.87, 137.10, 139.56, 140.82, 142.30, 148.64, 149.97, 168.16, and 170.00 (phenyl carbons of CNO−Cl ligand); 183.59 (metalated carbon); 208.28 (s, CO). ^{31}P NMR: 30.99 (s, 2PPh_3). IR: 1921 cm^{-1} (ν_{CO}).

Anal. Calcd for [Ru(PPh_3)$_2$(CO)(CNO−NO_2)]: C, 66.07; H, 4.29; N, 4.26. Found: C, 66.15; H, 4.80; N, 3.97. ^{1}H NMR:[8] 2.10 (CH_3); 4.95 (d, 1H, J = 9.0); 5.72 (s, 1H); 6.15 (d, J = 9.0); 6.01-(s, 1H); 7.20−7.70 (2PPh_3). ^{13}C NMR: 29.71 (s, CH_3); 127.71 (t, PPh_3, J = 16.70); 129.52 (s, PPh_3); 132.06 (t, PPh_3, J = 27.80); 134.02 (t, PPh_3, J = 22.30); 121.76, 129.10, 134.77, 139.56, 143.66, 143.88, 144.90, 149.19, 149.97, 169.26, and 171.20 (phenyl carbons of CNO−NO_2 ligand); 185.59 (metalated carbon); 208.31 (s, CO). ^{31}P NMR: 30.89 (s, 2PPh_3). IR: 1920 cm^{-1} (ν_{CO}).

Physical Measurements. Microanalyses (C, H, N) were performed using a Heraeus Carlo Erba 1108 elemental analyzer. IR spectra were obtained on a Perkin-Elmer 783 spectrometer with samples prepared as KBr pellets. Electronic spectra were recorded on a JASCO V-570 spectrophotometer. Magnetic susceptibilities were measured using a PAR 155 vibrating sample magnetometer fitted with a Walker Scientific L75FBAL magnet. NMR spectra were recorded in $CDCl_3$ solution with a Bruker AV 300 NMR spectrometer. ESR spectra were recorded with a Varian E-109C X-band spectrometer fitted with a quartz Dewar for measurements at 77 K (liquid dinitrogen). All ESR spectra were calibrated with an aid of DPPH (g = 2.0037). Electrochemical measurements were made using a CH Instruments model 600A electrochemical analyzer. A platinum disk working electrode, a platinum wire auxiliary electrode, and an aqueous saturated calomel reference electrode (SCE) were used in the cyclic voltammetry experiments. A platinum-wire gauge working electrode was used in the coulometric experiments. All electrochemical experiments were performed under a dinitrogen atmosphere. All electrochemical data were collected at 298 K and are uncorrected for junction potentials.

Crystallography. Single crystals of [Ru(PPh_3)$_2$(CO)(NO−OCH_3)(H)] and [Ru(PPh_3)$_2$(CO)(CNO−OCH_3)] were obtained by slow diffusion of hexane into dichloromethane solutions of the respective complexes. Selected crystal data and data collection parameters are given in Table 1. Data were collected, respectively, on a Nonius Kappa CCD diffractometer and a Bruker Smart Apex CCD diffractometer using graphite monochromated Mo Kα radiation (λ = 0.71073 Å) by ω scans. X-ray data reduction, structure

(8) Chemical shifts are given in ppm and multiplicity of the signals along with the associated coupling constants (J in Hz) are given in parentheses. Overlapping signals are marked with an asterisk.

Table 1. Crystallographic Data for $[Ru(PPh_3)_2(CO)(NO-OCH_3)(H)]$ and $[Ru(PPh_3)_2(CO)(CNO-OCH_3)]$

	$[Ru(PPh_3)_2(CO)(NO-OCH_3)(H)]\cdot H_2O$	$[Ru(PPh_3)_2(CO)-(CNO-OCH_3)]$
empirical formula	$C_{51}H_{46}N_2O_4P_2Ru$	$C_{51}H_{42}N_2O_3P_2Ru$
fw	913.91	893.88
space group	monoclinic, *C*2/*c*	triclinic, $P\bar{1}$
a, Å	36.6120(5)	11.1402(5)
b, Å	10.8869(2)	11.9230(5)
c, Å	22.6351(3)	17.4378(7)
α, deg	90	72.366(1)
β, deg	95.5736(5)	74.471(1)
γ, deg	90	80.368(1)
V, Å^3	8979.5(2)	2117.36(16)
Z	8	2
λ, Å	0.71073	0.71073
cryst size, mm^3	0.15 × 0.05 × 0.05	0.15 × 0.15 × 0.10
T, K	295(2)	295(2)
μ, mm^{-1}	0.467	0.492
R1[a]	0.0575	0.0579
wR2[b]	0.129	0.1222
GOF[c]	1.051	1.060

[a] $R1 = \sum||F_o| - |F_c||/\sum|F_o|$. [b] $wR2 = [\sum[w(F_o^2 - F_c^2)^2]/\sum[w(F_o^2)^2]]^{1/2}$. [c] $GOF = [\sum[w(F_o^2 - F_c^2)^2]/(M - N)]^{1/2}$, where *M* is the number of reflections and *N* is the number of parameters refined.

solution, and refinement were done using SHELXS-97 and SHELXL-97 programs.[9] The structure was solved by the direct methods.

Results and Discussion

Reaction of each 2-(arylazo)phenol (**1**) with $[Ru(PPh_3)_2(CO)_2Cl_2]$ has afforded two complexes with distinctly different colors, viz. red[10] and green, in comparable yields. Preliminary characterizations (microanalysis, IR, NMR, etc.), although gave some idea about the compositions of these two types of complexes, could not point to any definite formulation or stereochemistry of these complexes. For an unambiguous identification of these complexes, structure of a selected member from each family, viz. the red and green complexes obtained from the reaction with 2-(4′-methoxyphenylazo)-4-methylphenol (**1**, R = OCH_3), has been determined by X-ray crystallography. The structures are shown in Figures 1 and 2, and some selected bond parameters are given in Table 2.

Structure of the red complex (Figure 1) shows that the 2-(arylazo)phenol is coordinated to ruthenium, via dissociation of the phenolic proton, as a bidentate N,O-donor forming a five-membered chelate ring (**3**). Two triphenylphosphines, a carbon monoxide, and a hydride are also coordinated to the metal center. The red[10] complexes are therefore formulated in general as $[Ru(PPh_3)_2(CO)(NO-R)(H)]$, where NO−R refers to the N,O-coordinated 2-(arylazo)phenolate ligand (**3**). Microanalytical data of these $[Ru(PPh_3)_2(CO)(NO-R)(H)]$ complexes agree well with their compositions. The coordinated 2-(arylazo)phenolate ligand, CO, and hydride constitute one equatorial plane with the metal at the center (Figure 1b), where the CO is trans to the phenolate oxygen and the hydride is trans to the coordinated azo-nitrogen. The two PPh_3 ligands have taken up the remaining

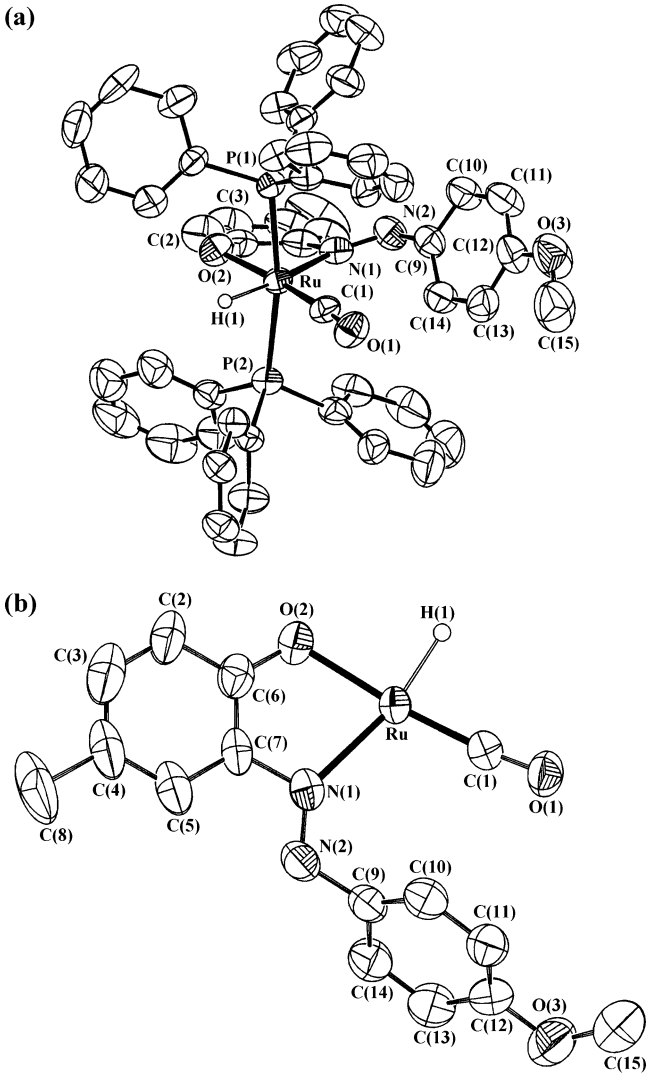

Figure 1. View of (a) the $[Ru(PPh_3)_2(CO)(NO-OCH_3)(H)]$ complex and (b) the equatorial plane.

two axial positions, and hence, they are mutually trans. The Ru−H, Ru−C, Ru−O, and Ru−P distances are all quite normal.[11] However, the Ru−N distance is found to be significantly longer than usual, and this elongation may be attributed to the strong trans effect of the coordinated hydride.[12] Structure of the green complex (Figure 2) shows that in this complex the 2-(arylazo)phenol is coordinated to the metal, via loss of the phenolic proton as well as another proton from one ortho position of the phenyl ring in the arylazo fragment, as a tridentate C,N,O-donor (**5**). The remaining three coordination sites are occupied by two triphenylphosphines and a carbon monoxide. The green complexes are therefore represented in general as $[Ru(PPh_3)_2(CO)(CNO-R)]$, where CNO−R stands for the C,N,O-coordinated 2-(arylazo)phenolate ligand (**5**). The observed microanalytical data of these $[Ru(PPh_3)_2(CO)(CNO-R)]$

(9) Sheldrick, G. M. *SHELXS-97 and SHELXL-97, Fortran programs for crystal structure solution and refinement*; University of Gottingen: Gottingen, Germany, 1997.

(10) Color of the $[Ru(PPh_3)_2(CO)(NO-NO_2)(H)]$ complex is purple.

(11) (a) Basuli, F.; Das, A. K.; Golam, M.; Peng, S. M.; Bhattacharya, S. *Polyhedron* **2000**, *19*, 1663. (b) Menon, M.; Pramanik, A.; Chattopadhyay, S.; Bag, N. Chakravorty, A. *Inorg. Chem.* **1995**, *34*, 1361. (c) Barral, M. C.; Aparicio, R. J.; Royer, E. C.; Saucedo, M. J.; Urbanos, F. A.; Puebla, E. G.; Valero, C. R. *J. Chem. Soc., Dalton Trans.* **1991**, 1609.

(12) Douglas, P. G.; Shaw, B. L. *J. Chem. Soc. A* **1970**, 1556.

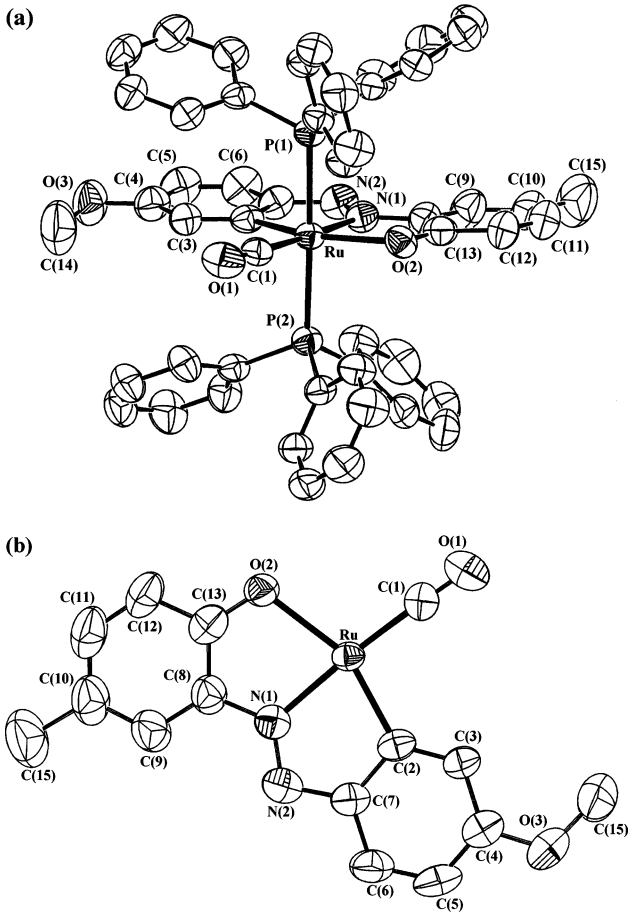

Figure 2. View of (a) the $[Ru(PPh_3)_2(CO)(CNO-OCH_3)]$ complex and (b) the equatorial plane.

Table 2. Selected Bond Distances and Bond Angles for $[Ru(PPh_3)_2(CO)(CNO-OCH_3)]$ and $[Ru(PPh_3)_2(CO)(NO-OCH_3)]$

$[Ru(PPh_3)_2(CO)(CNO-OCH_3)]$			
Bond Distances (Å)			
Ru−C(1)	1.865(4)	C(1)−O(1)	1.117(4)
Ru−C(2)	2.028(4)	N(1)−N(2)	1.286(4)
Ru−N(1)	2.034(3)	C(8)−N(1)	1.398(5)
Ru−O(2)	2.198(3)	C(7)−N(2)	1.401(5)
Ru−P(1)	2.3650(9)		
Ru−P(2)	2.3697(10)		
Bond Angles (deg)			
P(1)−Ru−P(2)	176.86(4)	C(2)−Ru−N(1)	78.00(15)
C(1)−Ru−N(1)	175.98(15)	N(1)−Ru−O(2)	78.17(12)
C(2)−Ru−O(2)	156.05(13)	Ru−C(1)−O(1)	177.4(4)
$[Ru(PPh_3)_2(CO)(NO-OCH_3)(H)]$			
Bond Distances (Å)			
Ru−H(1)	1.56(5)	C(1)−O(1)	1.163(6)
Ru−C(1)	1.816(6)	N(1)−N(2)	1.281(6)
Ru−N(1)	2.211(4)	C(7)−N(1)	1.432(7)
Ru−O(2)	2.113(4)	C(9)−N(2)	1.421(7)
Ru−P(1)	2.3590(15)		
Ru−P(2)	2.3570(15)		
Bond Angles (deg)			
P(1)−Ru−P(2)	168.24(5)	H(1)−Ru−O(2)	89.4(17)
C(1)−Ru−N(1)	107.9(2)	N(1)−Ru−O(2)	77.47(16)
H(1)−Ru−C(1)	85.2(17)	Ru−C(1)−O(1)	174.8(5)

complexes are consistent with their compositions. The coordinated 2-(arylazo)phenolate ligand and CO share an equatorial plane with the metal at the center (Figure 2b),

Scheme 1. Probable Steps for the Formation of $[Ru(PPh_3)_2(CO)(NO-R)(H)]$ and $[Ru(PPh_3)_2(CO)(CNO-R)]$ Complexes

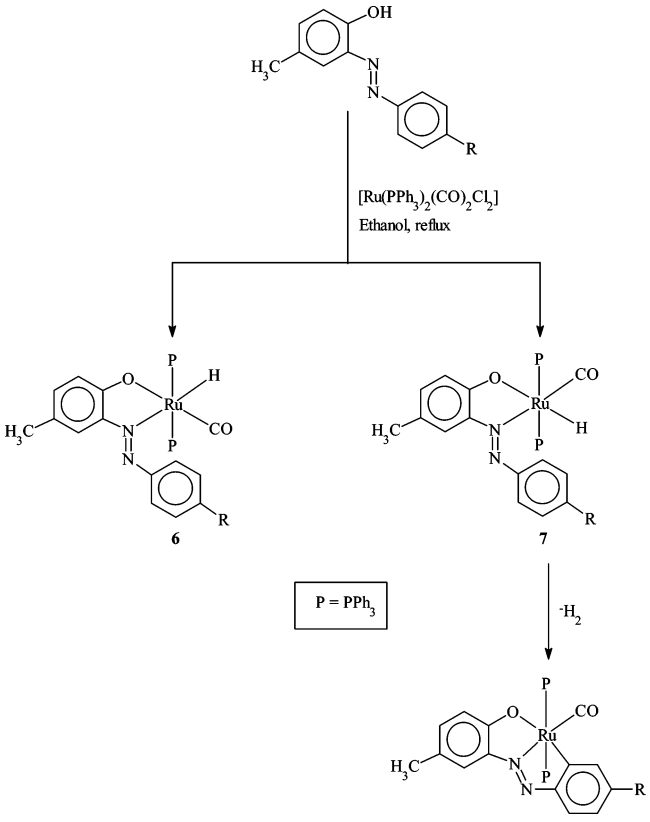

where the CO is trans to the coordinated azo-nitrogen. The PPh_3 ligands have occupied the axial positions as before. The bond parameters around the metal center are found to be quite normal.[11,3a] As all five complexes belonging to each group, viz. $[Ru(PPh_3)_2(CO)(NO-R)(H)]$ and $[Ru(PPh_3)_2(CO)(CNO-R)]$, have been synthesized similarly and they show similar spectroscopic and electrochemical properties (vide infra), the other four members of each group (with R $\neq OCH_3$) are assumed to have structures similar to those of their respective structurally characterized (R = OCH_3) analogues.

Formation of the two types of complexes, viz. $[Ru(PPh_3)_2(CO)(NO-R)(H)]$ and $[Ru(PPh_3)_2(CO)(CNO-R)]$, from the reaction of the 2-(arylazo)phenols (**1**) with $[Ru(PPh_3)_2(CO)_2Cl_2]$ in refluxing ethanol has been quite interesting. A careful examination of the equatorial plane of these two species, viz. $[Ru(PPh_3)_2(CO)(NO-R)(H)]$ and $[Ru(PPh_3)_2(CO)(CNO-R)]$, reveals that the relative disposition of the coordinated CO is different in the two types of complexes, which has also been interesting. The exact mechanism of formation of these two types of complexes is not completely clear to us. However, the sequences shown in Scheme 1 seem probable. In the initial step, the 2-(arylazo)phenol binds to the metal center, via displacement of a CO and elimination of HCl, as a bidentate N,O-donor. The remaining Ru−Cl bond is also converted to a Ru−H bond under the prevailing reaction conditions,[13] and thus, two isomers (**6** and **7**) of the [Ru-

(13) (a) Winter, R. F.; Hornung, F. M. *Inorg. Chem.* **1997**, *36*, 6197. (b) Young, R.; Wilkinson, G. *Inorg. Synth.* **1977**, *17*, 79. (c) Levison, J. J.; Robinson, S. D. *J. Chem. Soc. A* **1970**, 2947.

$(PPh_3)_2(CO)(NO-R)(H)]$ complexes are formed. In one of these two isomers (isomer **6**), the hydride is trans to the nitrogen and the CO is trans to the phenolate oxygen, while in other isomer (isomer **7**) relative disposition of the hydride and CO is the reverse. It appears that isomer **6** does not undergo any further reaction in refluxing ethanol, and hence, it is obtained as the red[10] $[Ru(PPh_3)_2(CO)(NO-R)(H)]$ complexes. In isomer **7**, the coordinated hydride is in the appropriate location to allow orthometalation of the pendent phenyl ring via elimination of molecular hydrogen, and this seems to have happened irreversibly to afford the green $[Ru(PPh_3)_2(CO)(CNO-R)]$ complexes. Rapid transformation of isomer **7** into the corresponding orthometalated species appears to have vitiated its isolation. This speculated scheme indicates that the isomer **6**, that is the red[10] $[Ru(PPh_3)_2(CO)(NO-R)(H)]$ complexes, cannot as such undergo any cyclometalation because of the inappropriate disposition of the hydride as well as CO. This scheme further indicates that isomerization of **6** to **7** could not take place in refluxing ethanol, presumably because of its relatively lower boiling point. To verify whether transformation of **6** to **7**, followed by the desired orthometalation, can take place at a higher (with respect to boiling ethanol) temperature, the red[10] $[Ru(PPh_3)_2(CO)(NO-R)(H)]$ complexes (isomer **6**) were simply treated in refluxing in 2-methoxyethanol (boiling point 125 °C), which indeed afforded the cyclometalated $[Ru(PPh_3)_2(CO)(CNO-R)]$ complexes in a quantitative yield. Furthermore, when direct reactions between $[Ru(PPh_3)_2(CO)_2Cl_2]$ and the 2-(arylazo)phenols (**1**) were carried out in refluxing 2-methoxyethanol, the cyclometalated green $[Ru(PPh_3)_2(CO)(CNO-R)]$ complexes were obtained as the sole product. All these results suggest that from the ethanol reaction the red[10] $[Ru(PPh_3)_2(CO)(NO-R)(H)]$ complex (**6**) as well as its geometrical isomer (**7**) are generated, probably via different kinetic routes. While the red complex (**6**) remains stable in refluxing ethanol, its isomer (**7**) undergoes rapid cyclometalation via elimination of H_2.[14] Isomerization of the red[10] complex **6** into complex **7**, followed by its rapid transformation into the cyclometalated product, takes place at a higher temperature.

Both the $[Ru(PPh_3)_2(CO)(NO-R)(H)]$ and $[Ru(PPh_3)_2(CO)(CNO-R)]$ complexes are found to be diamagnetic, which corresponds to the +2 state of ruthenium (low-spin d^6, $S = 0$) in these complexes. ^{1}H NMR spectra of the $[Ru(PPh_3)_2(CO)(NO-R)(H)]$ complexes show broad signals within 7.1−7.5 ppm for the coordinated PPh_3 ligands. The hydride signal is observed as a distinct triplet, due to coupling with the two magnetically equivalent phosphorus nuclei, near −10.5 ppm. The methyl signal from the phenolate fragment of the 2-(arylazo)phenolate ligand is observed near 2.0 ppm. Most of the expected signals from the aromatic protons of the coordinated 2-(arylazo)phenolate ligand have been clearly observed in all the complexes, while few could not be identified because of their overlap with the PPh_3 signals. Signals for the hydrogen containing substituents ($R = OCH_3$ and CH_3) in the arylazo fragment have also been observed in the expected region. Besides the absence of the hydride signal, the ^{1}H NMR spectrum of each $[Ru(PPh_3)_2(CO)(CNO-R)]$ complex is qualitatively similar to that of the corresponding $[Ru(PPh_3)_2(CO)(NO-R)(H)]$ complex. ^{13}C NMR spectra of the $[Ru(PPh_3)_2(CO)(NO-R)(H)]$ complexes show all the expected signals within 19.7−202.4 ppm, of which the signal near 19.74 ppm is assigned to the methyl carbon in the *para*-cresol fragment and the most deshielded signal near 202.4 ppm to the carbonyl carbon. ^{13}C NMR spectra of the $[Ru(PPh_3)_2(CO)(CNO-R)]$ complexes show all the expected signals within 29.7−208.4 ppm. The signal for the methyl carbon in the *para*-cresol fragment is observed near 29.7 ppm, and that for the carbonyl carbon is observed near 208.4 ppm. A distinct signal around 180 ppm is assigned to the metalated carbon of the CNO−R ligand. ^{31}P NMR spectra of all the complexes show a single resonance within 30−41 ppm, as expected. The NMR spectral data of the $[Ru(PPh_3)_2(CO)(NO-R)(H)]$ and $[Ru(PPh_3)_2(CO)(CNO-R)]$ complexes are therefore in well accordance with their respective composition and stereochemistry.

Infrared spectra of the $[Ru(PPh_3)_2(CO)(NO-R)(H)]$ complexes show many bands of different intensities below 2400 cm^{-1}. Assignment of each individual band to a specific vibration has not been attempted. However, in each of these complexes a sharp band is observed near 2360 cm^{-1}, which is assigned to the Ru−H stretching. Another strong band, observed around 1930 cm^{-1}, is assigned to the CO stretching. Three strong bands are displayed near 520, 695, and 745 cm^{-1}, which are attributable to the coordinated PPh_3 ligands. Comparison with the spectrum of $[Ru(PPh_3)_2(CO)_2Cl_2]$ shows the presence of some additional bands (near 1094, 1255, 1367, 1435, and 1479 cm^{-1}) in the spectra of the $[Ru(PPh_3)_2(CO)(NO-R)(H)]$ complexes, and these new bands are attributed to the coordinated 2-(arylazo)phenolate ligand. Besides the absence of the Ru−H stretch, the infrared spectrum of any $[Ru(PPh_3)_2(CO)(CNO-R)]$ complex is mostly very similar to that of the corresponding $[Ru(PPh_3)_2(CO)(NO-R)(H)]$ complex.

Both the $[Ru(PPh_3)_2(CO)(NO-R)(H)]$ and $[Ru(PPh_3)_2(CO)(CNO-R)]$ complexes are found to be poorly soluble in acetone and acetonitrile, but readily soluble in ethanol, 2-methoxyethanol, dichloromethane, and chloroform, producing intense red[10] and green solutions, respectively. Electronic spectra of complexes of both the types have been recorded in dichloromethane solution. All the complexes show intense absorptions in the visible and ultraviolet region (Table 3). The absorptions in the ultraviolet region are attributable to transitions within the ligand orbitals, and those in the visible region are probably due to allowed charge-transfer transitions. To have a better understanding of the nature of the transitions in the visible region, semiempirical EHMO calculations have been performed[15] on computer generated models of all the complexes, where phenyl rings of the triphenylphosphines are replaced by hydrogens. The

(14) The evolved hydrogen could not be detected experimentally.

(15) (a) Mealli, C.; Proserpio, D. M. *CACAO*, version 4.0; Italy, 1994. (b) Mealli, C.; Proserpio, D. M. *J. Chem. Educ.* **1990**, *67*, 399.

Table 3. Electronic Spectral and Cyclic Voltammetric Data

compd	electronic spectral data[a] λ_{max}/nm (ϵ, $M^{-1}\,cm^{-1}$)	cyclic voltammetric data[a,b] E, V vs SCE
$[Ru(PPh_3)_2(CO)(NO-OCH_3)(H)]$	514 (8500), 328 (14700)	0.73,[d] 1.18[d]
$[Ru(PPh_3)_2(CO)(NO-CH_3)(H)]$	508(7400), 322(15000)	0.76,[d] 1.24[d]
$[Ru(PPh_3)_2(CO)(NO-H)(H)]$	504(7000), 322(14500)	0.79,[d] 1.29[d]
$[Ru(PPh_3)_2(CO)(NO-Cl)(H)]$	518 (6000), 322(12900)	0.82,[d] 1.35[d]
$[Ru(PPh_3)_2(CO)(NO-NO_2)(H)]$	512 (9000), 326(17000)	0.92,[d] 1.36[d]
$[Ru(PPh_3)_2(CO)(CNO-OCH_3)]$	670 (7300), 390 (10500),[c] 356 (13000)	0.45[e] (70),[f] 1.13[e](80)[f]
$[Ru(PPh_3)_2(CO)(CNO-CH_3)]$	680 (2700), 422 (2500),[c] 356 (6000),	0.48[e] (90),[f] 1.00[d]
$[Ru(PPh_3)_2(CO)(CNO-H)]$	682 (5000), 428 (4800),[c] 354 (13000)	0.54[e] (70),[f] 1.40[d]
$[Ru(PPh_3)_2(CO)(CNO-Cl)]$	690 (1850), 424 (1450),[c] 360 (4000)	0.61[e] (70),[f] 1.39[d]
$[Ru(PPh_3)_2(CO)(CNO-NO_2]$	668 (6500), 428 (10000), 334 (8000)[c]	0.73[e] (60)[f]

[a] In dichloromethane. [b] Supporting electrolyte, TBAP; scan rate 50 mV s^{-1}. [c] Shoulder. [d] E_{pa} value. [e] $E_{1/2} = 0.5(E_{pa} + E_{pc})$. [f] $\Delta E_p = (E_{pa} - E_p)$, where E_{pa} and E_{pc} are anodic and cathodic peak potentials, respectively.

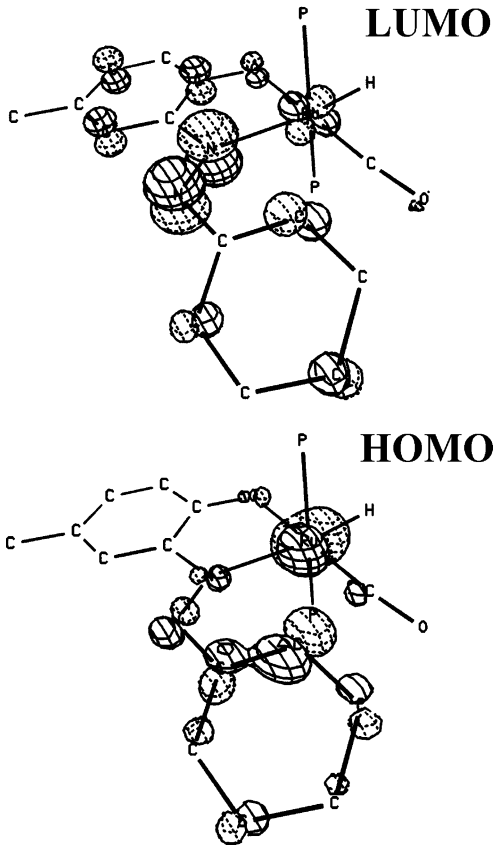

Figure 3. Partial molecular orbital diagram of the $[Ru(PPh_3)_2(CO)(NO-H)(H)]$ complex.

results of these calculations are found to be similar[16] for the five complexes in each group. Compositions of some selected molecular orbitals are given in Table S1, and a partial MO diagram of a representative $[Ru(PPh_3)_2(CO)(NO-R)(H)]$ complex is shown in Figure 3. A partial MO diagram of a selected $[Ru(PPh_3)_2(CO)(CNO-R)]$ complex is shown in Figure S1. In the $[Ru(PPh_3)_2(CO)(NO-R)(H)]$ complexes, the highest occupied molecular orbital (HOMO) has a major (>60%) contribution from the ruthenium d-orbitals, and the lowest unoccupied molecular orbital (LUMO) is delocalized almost entirely on the 2-(arylazo)phenolate ligand and is concentrated heavily (>50%)[16] on the azo (−N═N−) fragment. Hence, the intense absorption displayed around 510 nm by these $[Ru(PPh_3)_2(CO)(NO-R)(H)]$ complexes is assignable to the transition occurring from the filled ruthenium (t_2) orbital (HOMO) to the vacant π^*-(azo) orbital of the 2-(arylazo)phenolate ligand (LUMO). EHMO calculations of the $[Ru(PPh_3)_2(CO)(CNO-R)]$ complexes show a slightly different picture. The HOMOs of these complexes have comparable contributions from both the metal and the 2-(arylazo)phenolate ligand, but the LUMOs primarily consist of the azo fragment[16] as before. The lower energy (668−690 nm) absorption in the $[Ru(PPh_3)_2(CO)(CNO-R)]$ complexes is therefore attributed to the transition occurring from the filled HOMO (having both metal as well as ligand (CNO−R) character) to the vacant π^*-(azo) orbital of the 2-(arylazo)phenolate ligand (LUMO).

Electrochemical properties of both the $[Ru(PPh_3)_2(CO)(NO-R)(H)]$ and $[Ru(PPh_3)_2(CO)(CNO-R)]$ complexes have been studied by cyclic voltammetry in 1:9 dichloromethane−acetonitrile solution (0.1 M TBAP).[17] The voltammetric data are given in Table 3, and a selected voltammogram is deposited as Supporting Information (Figure S2). Complexes of both types show two oxidative responses on the positive side of SCE. In the $[Ru(PPh_3)_2(CO)(NO-R)(H)]$ complexes, the first oxidative response, observed within 0.73−0.90 V,[18] is irreversible in nature, and in view of the composition of the HOMO (vide infra) this oxidation is assigned to the Ru(II)−Ru(III) oxidation. However, in the $[Ru(PPh_3)_2(CO)(CNO-R)]$ complexes the first oxidation, observed within 0.46−0.73 V, is reversible in nature, characterized by a peak-to-peak separation (ΔE_p) of 70 mV, which remains unchanged upon changing the scan rate, and the anodic peak current (i_{pa}) is almost equal to the cathodic peak current (i_{pc}) as expected for a reversible electron-transfer process. In view of the composition of the HOMO in these complexes (vide supra), assignment of the oxidation to the metal center alone seemed unjustified. For a satisfactory assignment of this oxidation, each $[Ru(PPh_3)_2(CO)(CNO-R)]$ complex was coulometrically oxidized at an appropriate (E_{pa} + 0.2 V) potential. The oxidations have been smooth and quantitative, associated with a color change of green to brownish-green (brown for R = NO_2). ESR spectra recorded on the oxidized solutions show sharp and

(16) In the case of R = NO_2, the LUMOs of both the types of complexes have a considerable contribution (>45%) from the nitro group.

(17) A little dichloromethane was necessary to take the complex into solution. Addition of large excess of acetonitrile was necessary to record the redox responses in proper shape.

(18) Potentials are recorded with reference to SCE.

nearly isotropic signals with $g \sim 2.0$. The signals are representative of free radicals with very little anisotropic effect arising from the metal center. This result corresponds well with the composition of the HOMO in such species. The site of the first oxidation in the $[Ru(PPh_3)_2(CO)(NO-R)(H)]$ complexes could not be verified because of the irreversible nature of this oxidation.

The potential of the irreversible Ru(II)−Ru(III) oxidation in the $[Ru(PPh_3)_2(CO)(NO-R)(H)]$ complexes has been found to be sensitive to the nature of the substituent R in the arylazo fragment. The potential increases with increasing electron-withdrawing character of the substituent R. The plot of oxidation potential versus σ [σ = Hammett *para* substituent constant of R;[19] $OCH_3 = -0.27$, $CH_3 = -0.17$, H = 0.00, Cl = 0.23, and $NO_2 = 0.78$] is found to be linear (Figure S3) with a slope (ρ) of 0.17 V (ρ = reaction constant of this couple[20]), which shows that the nature of *para*-substituent R on the 2-(arylazo)phenolate ligand, which is seven bonds away from the metal center, can still influence the metal-centered oxidation potential in a predictable manner. The potential of the reversible oxidation in the $[Ru(PPh_3)_2(CO)(CNO-R)]$ complexes also shows a linear dependence on the electronic nature of the substituent R (Figure S4) with a considerably higher slope ($\rho = 0.27$ V). The observed higher value of ρ may be attributed to the combined effect of closeness of R to the metal center (four bonds away) and larger contribution of ligand (CNO−R) in the redox active HOMO. The second oxidative response, displayed by the $[Ru(PPh_3)_2(CO)(NO-R)(H)]$ and $[Ru(PPh_3)_2(CO)(CNO-R)]$ complexes, above 1.1 V, is irreversible in nature and is tentatively assigned to a ligand (NO−R or CNO−R) centered oxidation. The potential of this irreversible oxidation does not show any systematic variation with the nature of the substituent R.

(19) Hammett, L. P. *Physical Organic Chemistry*, 2nd ed.; McGraw-Hill: New York, 1970.
(20) Mukherjee, R. N.; Rajan, O. A.; Chakravorty, A. *Inorg. Chem.* **1982**, *21*, 785.

Conclusion

The present study shows that $[Ru(PPh_3)_2(CO)_2Cl_2]$ can successfully mediate C−H activation of the 2-(arylazo)-phenols (**1**). This study also indicates that similar bond activation of organic molecules that have structural similarity with the 2-(arylazo)phenols (**1**) should also be possible upon their reaction with $[Ru(PPh_3)_2(CO)_2Cl_2]$, and such possibilities are currently under exploration.

Acknowledgment. The authors thank the reviewers for their comments and suggestions, which have been helpful in preparing the revised version of the manuscript. Financial assistance received from the Department of Science and Technology [Grant SR/S1/IC-15/ 2004] is gratefully acknowledged. The authors thank the RSIC at Central Drug Research Institute, Lucknow, India, for the C,H,N analysis data. S.D thanks the CSIR, New Delhi, for her fellowship [Grant No. 9/96(410)/2003-EMR-I].

Supporting Information Available: Partial molecular orbital diagram of $[Ru(PPh_3)_2(CO)(CNO-H)]$ (Figure S1), cyclic voltammogram of $[Ru(PPh_3)_2(CO)(CNO-OCH_3)]$ (Figure S2), least-squares plots of E_{pa} values of Ru(II)−Ru(III) couple versus σ for the $[Ru(PPh_3)_2(CO)(NO-R)(H)]$ complexes (Figure S3), least-squares plots of $E_{1/2}$ values of Ru(II)−Ru(III) couple versus σ for the $[Ru(PPh_3)_2(CO)(CNO-R)]$ complexes (Figure S4),^{1}H NMR spectrum of $[Ru(PPh_3)_2(CO)(NO-H)(H)]$ (Figure S5), molecular orbital interaction diagram of $[Ru(PPh_3)_2(CO)(NO-CH_3)(H)]$ (Figure S6), composition of selected molecular orbitals for all the complexes (Table S1), and X-ray crystallographic data in CIF format.This material is available free of charge via the Internet at http://pubs.acs.org.

IC051874V